Effect of the mechanical oscillator on the optical-response properties of an optical trimer system

Xiyun Li,[1] Wenjie Nie,[1,*] Aixi Chen,[2,†] and Yueheng Lan[3,‡]
[1]*Department of Applied Physics, East China Jiaotong University, Nanchang 330013, China*
[2]*Department of Physics, Zhejiang Sci-Tech University, Hangzhou 310018, China*
[3]*Department of Physics, Beijing University of Posts and Telecommunications, Beijing 100876, China*

(Received 10 August 2018; published 27 November 2018)

We propose theoretically a four-mode coupled optomechanical system to explore the optical-response properties of an optical trimer system consisting of a passive cavity, a no-loss-gain cavity, and an active cavity coupled with a mechanical oscillator. In the study, the passive cavity is driven by an external laser so that the stability of the coupled system depends strongly on the gain-to-loss ratio and the photon tunneling between the adjacent cavities. We find that in the regime near the stable-unstable critical point, the resonance absorption of the optical trimer system changes quickly with the increasing gain of the active cavity. In contrast, when the mechanical oscillator is coupled to the passive cavity, the center absorption peak is split and a phenomenon of optomechanically induced transparency appears. Consequently, two additional resonance peaks in the absorption profile are induced by the optomechanical coupling, which hinges on the tunneling between the optical cavities and also on the gain of the active cavity. The dependence of the width of the transparency window on the optomechanical coupling and the driving strength is also discussed in detail. The results obtained here indicate that the optical properties of the trimer system can be manipulated by coupling a mechanical oscillator to the system and therefore have a potential application in quantum optics and quantum information processing.

DOI: 10.1103/PhysRevA.98.053848

I. INTRODUCTION

Recently, cavity optomechanics, exploring a significant interaction between electromagnetic fields and mechanical systems via radiation pressure, has received extensive attention [1–3]. It provides a reliable platform to study theoretically and experimentally the control of mechanical motion at the quantum level, such as the coherence and entanglement of a macroscopic mechanical oscillator and a cavity field [4–7], the cooling of mechanical vibrations to quantum ground states [8–12], and the nonlinear quantum effects in quantum optomechanics [13–19]. Moreover, the quantum nature of a moving mirror in the context of quantum optomechanics can be probed by a single photon [20,21]. The optomechanical interaction leads to the phenomena of optomechanically induced transparency (OMIT) [22–27] and absorption (OMIA) [28–30]. They are analogs of electromagnetically induced transparency [31–33] and absorption [34–38] that originate from the internal destructive or constructive interference of atom-field coupled systems. By adjusting the width of transparent windows, OMIT can be used to control the propagation of a light field [39–42]. OMIT and OMIA have many applications in quantum information and communication, such as slow light [24,42,43], optical storage [40,41,44], charge measurement [45], single photon routers [46], and so on. It has been demonstrated that OMIA can exist in a microdisk optomechanical resonator with silicon nitride [47]. In particular, the combination of OMIA and OMIT has potential applications in photocurrent switches [28,48].

Based on a typical optical system of a Fabry-Pérot cavity [22,49], the role of various nonlinear media in coupled optomechanical systems has been discussed. For example, a quantum two-level system (qubit) is introduced into the cavity to enhance the radiation-pressure interaction and nonlinearity of the system [50–52]. The influence of dipole-dipole interacting atoms on the single-photon spectrum of a hybrid system with a strong atom-cavity coupling as well as strong optomechanical interactions is also investigated in detail [52]. In addition, a degenerate optical parametric amplifier (OPA) and a higher order excited atomic medium are disposed in the Fabry-Pérot cavity to achieve tunable slow and fast light [53]; a nanosphere suspended in the cavity is used to control the optical-response properties of the system [54]; and a single atom is trapped in the cavity to realize an effective coupling between the micromachined cantilever and the cavity field [55]. Further, the effective nonlinear coupling between the optical gain cavity and mechanical modes [56,57] and the photon-induced tunneling effect [15,58,59] are analyzed in detail in optomechanical systems, where most studies of OMIT have been understood in terms of two coupled oscillators [60]. The adjacent cavities in an optomechanical system enable two pathways' interference [22,24,61], which can also be manipulated by the gain photons tunneling between them [62]. In this regard, a series of research efforts on coupled cavities—such as studies of slow light and the transparency induced by a coupled resonator in two coupled signal-cavity modes [62], PT symmetric phase transition and photonic transmission in an optical trimer system [63], optomechanically induced transparency in a multicavity

*niewenjiezhu@sina.cn
†aixichen@163.com
‡lanyh@bupt.edu.cn

optomechanical system [64], and tunable optomechanically induced transparency and absorbtion in a hybrid optomechanical system consisting of two cavities and a mechanical oscillator [29,65] or membrane [66]—have been put forward; these can demonstrate the quantum coherence effects in a hybrid optomechanical system. Moreover, the tunneling between two optical cavities can be mediated by a mechanical mode, which helps amplify the single-photon coupling strength [67].

In this study, similar to the previous work on two coupled cavities interacting with a mechanical mode [65], a four-mode coupled optomechanical system composed of a mechanical oscillator and an optical trimer system [63] is built to explore the optomechanical coupling in the system. Compared with a two-cavity system coupled to a mechanical oscillator, the tunneling of photons in the optical trimer system bestows the system with more interference channels. Furthermore, the optical response in the optomechanical system can be controlled by changing two tunneling strengths between the no-loss-gain cavity and the adjacent cavities as well as the gain of the active cavity. In particular, we can explore the optical-response properties of the system approaching a stable-unstable critical value by analyzing the stability characteristics of the system, which depends on the external control parameter of the system. To this end, we first compute the Lyapunov exponents to obtain the boundaries of the stable and unstable regimes of the system in the presence or the absence of optomechanical coupling. Subsequently, we analyze the optical properties of the probe field and check the two discovered transparency windows, which can be controlled by adjusting the values of the tunneling strengths between adjacent cavities and the gain of the active cavity. In particular, in the regime approaching the stable-unstable critical point, a strong resonance absorption appears with increasing gain of the active cavity. When the mechanical oscillator is coupled to the passive cavity of the trimer system, we find that the anti-Stokes field caused by the mechanical resonator can induce one type of transparency due to the split of the middle absorption peak in the absorption profile; and the positions of the far left and right absorption peaks can be adjusted by changing the effective optomechanical coupling. Finally, we also discuss in detail the effect of the system's driving strength on the optical properties of the four-mode optomechanical system.

The paper is organized as follows. In Sec. II, the model and its Hamiltonian are described. In Sec. III, the quantum Langevin equation is derived and linearized to obtain the dynamics of the quantum fluctuations around the steady-state mean values. Further, the border of the stable and unstable regimes of the coupled system is evaluated numerically and the output field at the probe frequency is computed. In Sec. IV, we analyze in detail the effect of the mechanical oscillator on the optical-response properties of the optical trimer system. The paper is concluded in Sec. V.

II. MODEL

As depicted in Fig. 1, our model is a four-mode coupled optomechanical system consisting of an array of three single-mode cavities and a mechanical oscillator. The main aim is to investigate the effect of the mechanical oscillator on the optical properties of the optical trimer system [63]. Here the first cavity is passive and the loss rate and the resonance frequency of the cavity are, respectively, γ_1 and ω_{c1}; the middle cavity is a no-loss-gain cavity and its resonance frequency is ω_{c0}; the third cavity is a gain optical cavity with gain rate γ_2 and resonance frequency ω_{c2}. In the three-cavity subsystem, we only consider the photon tunnelings between two adjacent cavities. Correspondingly, the photon-tunneling strengths are, respectively, J_1 and J_2, which can be adjusted by changing the distance between adjacent cavities [29,62,63]. In addition, the quantum mechanical oscillator (with mass m and decay rate γ_m) interacts with the passive cavity with optomechanical coupling strength g_1, where the passive cavity is driven by a strong driving field with amplitude Ω_d and frequency ω_d as well as a weak probe field with amplitude ε_p and frequency ω_p. The total Hamiltonian of the system reads

$$H_t = H_0 + H_{in} + H_d + H_p, \tag{1}$$

where

$$\begin{aligned} H_0 &= \omega_{c1}a_1^\dagger a_1 + \omega_{c0}a_0^\dagger a_0 + \omega_{c2}a_2^\dagger a_2 + \omega_m b^\dagger b, \\ H_{in} &= J_1(a_0^\dagger a_1 + \text{H.c.}) + J_2(a_0^\dagger a_2 + \text{H.c.}) - g_1 a_1^\dagger a_1(b^\dagger + b), \\ H_d &= i(a_1^\dagger \Omega_d\, e^{-i\omega_d t} - a_1 \Omega_d^*\, e^{i\omega_d t}), \\ H_p &= i(a_1^\dagger \varepsilon_p\, e^{-i\omega_p t} - a_1 \varepsilon_p^*\, e^{i\omega_p t}). \end{aligned} \tag{2}$$

Here a_1, a_0, a_2, and b are the annihilation operators belonging to the passive cavity, the no-loss-gain cavity, the gain cavity, and the mechanical oscillator, respectively. H_0 denotes the free Hamiltonian of the cavities and the mechanical oscillator, and H_{in} denotes the interaction Hamiltonian in the system. H_d and H_p describe the interaction of the passive cavity mode with the driving field with amplitude $|\Omega_d| = \sqrt{\frac{2P_d\gamma_1}{\hbar\omega_d}}$ and the probe field with amplitude $|\varepsilon_p| = \sqrt{\frac{2P_p\gamma_1}{\hbar\omega_p}}$, respectively. P_d and P_p are the driving and probe laser powers.

Further, considering the rotating-wave approximation of the system and combining the transformation $H \to U^\dagger H_t U - iU^\dagger \partial_t U$ written into the interaction picture with respect to $U = \exp[-i\omega_d(a_1^\dagger a_1 + a_0^\dagger a_0 + a_2^\dagger a_2)t]$, we obtain the Hamiltonian afresh,

$$\begin{aligned} H = {} & \Delta_{c1}a_1^\dagger a_1 + \Delta_{c0}a_0^\dagger a_0 + \Delta_{c2}a_2^\dagger a_2 + \omega_m b^\dagger b \\ & - g_1 a_1^\dagger a_1(b^\dagger + b) + J_1(a_0^\dagger a_1 + \text{H.c.}) + J_2(a_0^\dagger a_2 + \text{H.c.}) \\ & + i(a_1^\dagger \varepsilon_p\, e^{-i\delta t} - a_1 \varepsilon_p^*\, e^{i\delta t}) + i(a_1^\dagger \Omega_d - a_1 \Omega_d^*), \end{aligned} \tag{3}$$

where $\Delta_{ci} = \omega_{ci} - \omega_d$ $(i = 0, 1, 2)$ represents the cavity-pump detuning between the driving and cavity fields; $\delta = \omega_p - \omega_d$ is the detuning resulting from the probe and the driving field.

III. QUANTUM DYNAMICS AND FLUCTUATIONS

For the convenience of studying the dynamics of the system, we define the dimensionless position operator $x = \frac{b+b^\dagger}{\sqrt{2}}$ and the dimensionless momentum operator $p = \frac{b-b^\dagger}{\sqrt{2}i}$ for Eq. (3). According to the Heisenberg equation, we obtain the following nonlinear dynamic equations of the system when

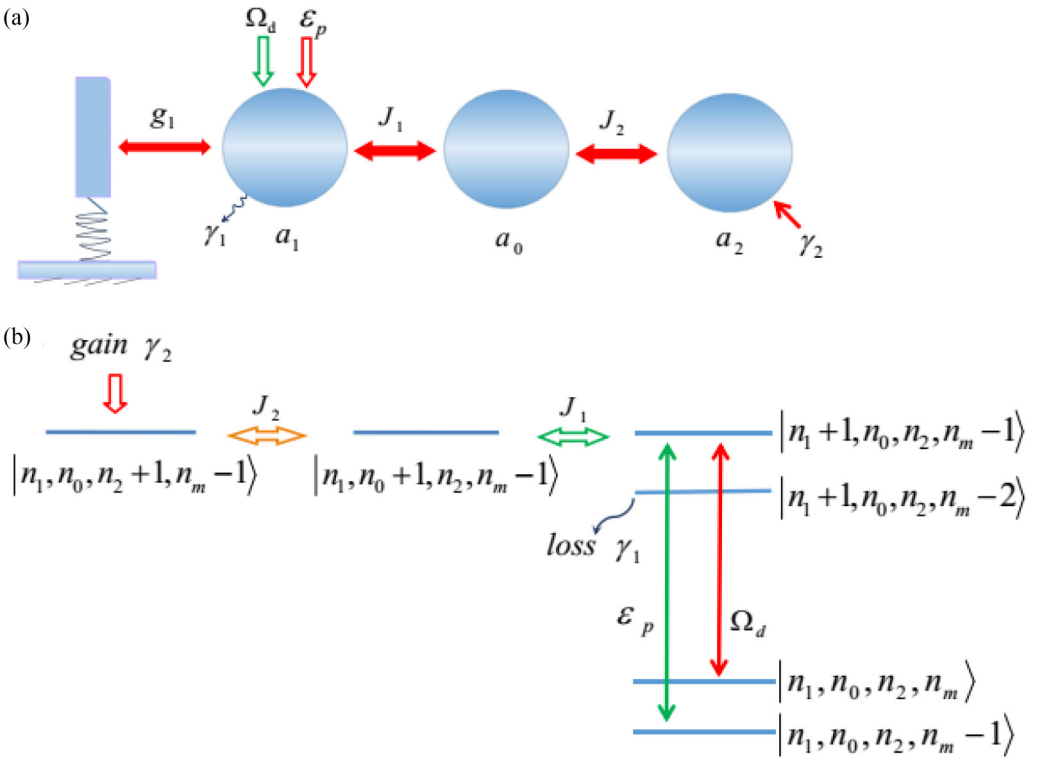

FIG. 1. (a) Schematic illustration of a four-mode coupled optomechanical system consisting of an array of three single-mode cavities and a mechanical oscillator. In this setup, the mechanical oscillator and the optical cavity (a_0) without loss and gain simultaneously couple to the passive cavity (a_1), which is driven by an external laser field with the strength Ω_d and a weak probe field with the strength ε_p. In addition, the cavity a_0 interacts with an active cavity (a_2). (b) Energy level diagram of the system. $|n_1, n_0, n_2, n_m\rangle$ denotes the state of $n_{1,0,2}$ photons in the three optical modes and n_m phonons in the mechanical mode.

the mechanical oscillator couples to the passive cavity:

$$\begin{aligned}
&\dot{x} = \omega_m p, \quad \dot{p} = -\frac{\gamma_m}{2} p - \omega_m x + \sqrt{2} g_1 a_1^\dagger a_1, \\
&\dot{a_1} = \left(-i\Delta_{c1} - \frac{\gamma_1}{2}\right) a_1 + i\sqrt{2} g_1 a_1 x - i J_1 a_0 + \Omega_d + \varepsilon_p\, e^{-i\delta t}, \\
&\dot{a_2} = \left(-i\Delta_{c2} + \frac{\gamma_2}{2}\right) a_2 - i J_2 a_0, \\
&\dot{a_0} = -i\Delta_{c0} a_0 - i J_1 a_1 - i J_2 a_2,
\end{aligned} \tag{4}$$

where the dimensionless position and momentum operators of the mechanical oscillator, x and p, satisfy the commutation relation $[x, p] = i$. We focus mainly on the mean response of the coupled system to the probe field, with the quantum noise of the cavity field and the thermal noise being neglected in Eq. (4). It is noted that the stability of the coupled system should be investigated in detail because the system is driven by an laser. We first derive the dynamics of the quantum fluctuations in the system by using Eq. (4). Considering the perturbation made by the probe field, we decompose each operator as the sum of its steady-state value and a small fluctuation, i.e., $O = O_s + \delta O$ ($O = x, p, a_i$), and further split the cavity modes into real and imaginary parts, i.e., $a_i = \mathrm{Re}[a_{is}] + i\,\mathrm{Im}[a_{is}] + \delta\,\mathrm{Re}[a_i] + i\delta\,\mathrm{Im}[a_i]$. By inserting the ansatz above into Eq. (4) and neglecting all higher order terms and the probe term $\varepsilon_p\, e^{-i\delta t}$, we obtain the quantum dynamics for these fluctuations of the system. For simplicity, we write it into a more compact form $\dot{f}(t) = Af(t)$, where the column vector of the fluctuation operator is $f^T(t) = (\delta x(t), \delta p(t), \delta\,\mathrm{Re}[a_1](t), \delta\,\mathrm{Im}[a_1](t), \delta\,\mathrm{Re}[a_2](t), \delta\,\mathrm{Im}[a_2](t), \delta\,\mathrm{Re}[a_0](t), \delta\,\mathrm{Im}[a_0](t))$ and the drift matrix A containing the stability characterization is

$$A = \begin{pmatrix}
0 & \omega_m & 0 & 0 & 0 & 0 & 0 & 0 \\
-\omega_m & -\frac{\gamma_m}{2} & 2\sqrt{2} g_1\,\mathrm{Re}[a_{1s}] & 2\sqrt{2} g_1\,\mathrm{Im}[a_{1s}] & 0 & 0 & 0 & 0 \\
-\sqrt{2} g_1\,\mathrm{Im}[a_{1s}] & 0 & -\frac{\gamma_1}{2} & \Delta_{c1} - \sqrt{2} g_1 x_s & 0 & 0 & 0 & J_1 \\
\sqrt{2} g_1\,\mathrm{Re}[a_{1s}] & 0 & -\Delta_{c1} + \sqrt{2} g_1 x_s & -\frac{\gamma_1}{2} & 0 & 0 & -J_1 & 0 \\
0 & 0 & 0 & 0 & \frac{\gamma_2}{2} & \Delta_{c2} & 0 & J_2 \\
0 & 0 & 0 & 0 & -\Delta_{c2} & \frac{\gamma_2}{2} & -J_2 & 0 \\
0 & 0 & 0 & J_1 & 0 & J_2 & 0 & \Delta_{c0} \\
0 & 0 & -J_1 & 0 & -J_2 & 0 & -\Delta_{c0} & 0
\end{pmatrix}, \tag{5}$$

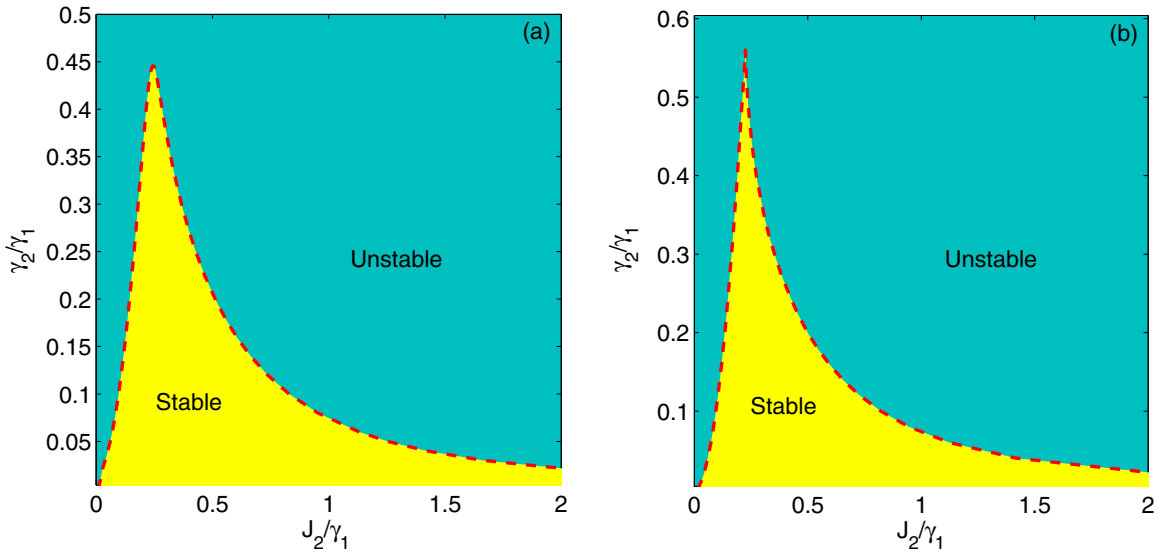

FIG. 2. The contour of the largest Lyapunov exponent versus the tunneling strength J_2/γ_1 and the gain-to-loss ratio γ_2/γ_1 with and without the optomechanical coupling g_1. The yellow area denotes the system's stable regime and the blue area shows the unstable regime. The red dashed line stands for the border between the stable and unstable regimes. The parameter values we selected are $\gamma_1 = 2\pi \times 10^6$, $\omega_m = 23.4\gamma_1$ Hz, $\gamma_m = 0.038\gamma_1$, $\Delta_{ci} = \omega_m$ $(i = 0, 1, 2)$, $J_1 = 0.3\gamma_1$, $\Omega_d = 10^5\gamma_1$. (a) $g_1 = 2.1 \times 10^{-5}\gamma_1$, (b) $g_1 = 0$.

where x_s and a_{1s} are, respectively, the steady-state expectation values of the mechanical oscillator and the passive cavity field, which can be obtained by setting the time derivatives to 0 in Eq. (4). We also assumed a large number of photons in the passive cavity, i.e., $|a_{1s}| \gg 1$.

It is known that the real parts of the eigenvalues of the drift matrix are the Lyapunov exponents of this nonlinear dynamical system [68–70]. If all the Lyapunov exponents are negative, then the mean-value trajectories of the system tend to a fixed point in the phase space. However, as long as one of these Lyapunov exponents is positive, the system will become unstable [69,71]. We can numerically evaluate all the Lyapunov exponents of the optomechanical system through the drift matrix A. However, we only need to focus on the largest Lyapunov exponent of the system, which can be regarded as an indicator to distinguish the stable and unstable regimes of the system. This is because when its value becomes positive, the stability condition of the system is broken and thus the system enters the unstable region. Accessible parameters of the cavity are selected, i.e, the decay rate of the passive cavity is $\gamma_1 = 2\pi \times 10^6$ Hz, corresponding to a Q factor $Q_c \sim 3 \times 10^7$ of the passive cavity, the cavity-pump detuning between the driving field, and the cavity fields $\Delta_{ci} = \omega_m$ $(i = 0, 1, 2)$ [72–74]. The mechanical oscillation frequency is $\omega_m = 23.4\gamma_1$, the damping rate is $\gamma_m = 0.038\gamma_1$, and the driving amplitude is $\Omega_d = 10^5\gamma_1$ [74–77]. The tunneling strength between the passive cavity and the no-loss-gain cavity is $J_1 = 0.3\gamma_1$, and depends on the distance between adjacent cavities [29,62,63]. In addition, the order of magnitude of the optomechanical coupling is generally 100 Hz [1]. Here we select $g_1 = 2.1 \times 10^{-5}\gamma_1$.

Using above parameters, in Fig. 2 we plot the largest Lyapunov exponent as a function of the tunneling strength J_2/γ_1 and the gain-to-loss ratio γ_2/γ_1 in the presence or the absence of the optomechanical coupling g_1, where the yellow area denotes the stable regime, the blue area denotes the unstable regime, and the red dashed line stands for the border between the stable and unstable regimes. It is found from Fig. 2 that, in the two cases, for the coupling strength J_2 there exist a minimum value $J_2^{\min}$ and a maximum value $J_2^{\max}$ for each fixed γ_2/γ_1, at which the system can be transformed from the stable to the unstable state. The width of the stable interval of J_2, i.e., $\Delta J_2 = J_2^{\max} - J_2^{\min}$, decreases with increasing gain-to-loss ratio γ_2/γ_1. Further, we see from Figs. 2(a) and 2(b) that the left border between the stable and unstable regimes does not change significantly when the optomechanical coupling and the gain-to-loss ratio are relatively small. In particular, in the condition of approaching a balanced gain-to-loss ratio, i.e., $\gamma_2 \to \gamma_1$, the largest Lyapunov exponents are always positive and therefore the optical trimer system and the four-mode coupled optomechanical system are always unstable. In Fig. 3, we also plot the border line as a function of the tunneling strength J_2/γ_1 and the gain-to-loss ratio γ_2/γ_1 with different optomechanical couplings g_1. It is found from Fig. 3 that, for a given γ_2/γ_1, the finite stable interval ΔJ_2 moves to the right with increasing optomechanical coupling. In the following, we mainly study the optical properties of the optical trimer system in the stable regime and the effect of the mechanical oscillator on the optical properties of the optomechanical coupled system. Especially, the change of the absorption shape of the system approaching the border of stable and unstable regimes can be discussed.

In order to investigate the mean response of the system to the probe field, we expand the steady-state solution of Eq. (4) that contains many Fourier components and neglect the high-order terms of ε_p in the limit of weak probe field. Then, the form of each operator can be written as [23,74,78]

$$O = O_s + {}^{+}O\varepsilon_p\, e^{-i\delta t} + {}^{-}O\varepsilon_p^*\, e^{i\delta t}, \tag{6}$$

$$\dot{O} = -i\delta\, {}^{+}O\varepsilon_p\, e^{-i\delta t} + i\delta\, {}^{-}O\varepsilon_p^*\, e^{i\delta t}. \tag{7}$$

Substituting Eqs. (6) and (7) into Eq. (4) and comparing the coefficients of $e^{i\delta t}$ and $e^{-i\delta t}$ on the two sides of the equation, the steady-state solutions and the amplitudes of the first-order sidebands of this coupled optomechanical system can be derived, i.e.,

$$x_s = \frac{\sqrt{2}g_1|a_{1s}|^2}{\omega_m}, \quad a_{1s} = \frac{\Omega_d}{i\Delta_1 + \frac{\gamma_1}{2} - \frac{J_1^2(-i\Delta_{c2}+\frac{\gamma_2}{2})}{J_2^2 - i\Delta_{c0}(-i\Delta_{c2}+\frac{\gamma_2}{2})}}, \tag{8}$$

and

$${}^{+}a_1 = \frac{\omega_m^2 - \delta^2 - i\delta\gamma_m/2 + \frac{\beta_1}{-i(\Delta_1+\delta-R)+\frac{\gamma_1}{2}}}{\left[\omega_m^2 - \delta^2 - i\delta\gamma_m/2 + \frac{\beta_1}{-i(\Delta_1+\delta-R)+\frac{\gamma_1}{2}}\right]\left[i(\Delta_1-\delta-Q)+\frac{\gamma_1}{2}\right] - \beta_1}, \tag{9}$$

where the undefined variables are $\beta_1 = i\sqrt{2}g_1\omega_m^2 x_s$, $\Delta_1 = \Delta_{c1} - \sqrt{2}g_1 x_s$, $R = \frac{J_1^2}{(\Delta_{c0}+\delta)+iB}$, $Q = \frac{J_1^2}{(\Delta_{c0}-\delta)-iM}$, $M = \frac{J_2^2}{i(\Delta_{c2}-\delta)-\frac{\gamma_2}{2}}$, $B = \frac{J_2^2}{-i(\Delta_{c2}+\delta)-\frac{\gamma_2}{2}}$. We have ignored those terms containing ε_p^2, ε_p^{*2}, and $|\varepsilon_p|^2$. Further, we write the input-output relation of this coupled optomechanical system as

$$\varepsilon_{\text{out}}(t) + \varepsilon_p\, e^{-i\delta t} + \Omega_d = \gamma_1 a_1. \tag{10}$$

Expanding the output field $\varepsilon_{\text{out}}(t)$ as $\varepsilon_{\text{out}}(t) = \varepsilon_{\text{out}}^s(t) + {}^{+}\varepsilon_{\text{out}}(t)\varepsilon_p\, e^{-i\delta t} + {}^{-}\varepsilon_{\text{out}}(t)\varepsilon_p^*\, e^{i\delta t}$ and substituting it into the above equation, we obtain the output transmission spectra as follows:

$$\varepsilon_{\text{out}}^s = \gamma_1 a_{1s} - \Omega_d, \quad {}^{+}\varepsilon_{\text{out}} = \gamma_1 {}^{+}a_1 - 1, \quad {}^{-}\varepsilon_{\text{out}} = \gamma_1 {}^{-}a_1. \tag{11}$$

In order to analyze the optical response of the whole system to the weak probe field, we write the amplitude of the rescaled output field corresponding to the weak probe field as, i.e., $\chi = {}^{+}\varepsilon_{\text{out}} + 1 = \gamma_1 {}^{+}a_1$ [74]; the real and imaginary parts of χ describe the absorption and the dispersion of the probe field, respectively [23]. When the real part $\text{Re}(\chi) \to 0$ and the imaginary part $\text{Im}(\chi) \to 0$ are simultaneously satisfied, an OMIT window will appear [79].

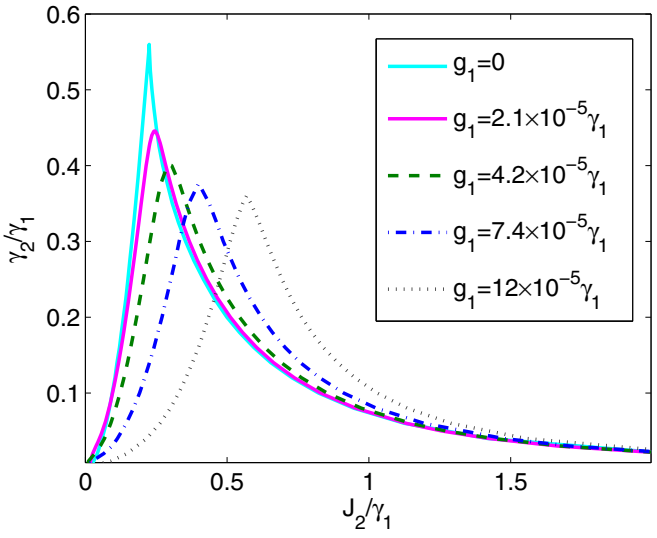

FIG. 3. The border lines between the stable and unstable regimes as a function of the tunneling strength J_2/γ_1 and the gain-to-loss ratio γ_2/γ_1 with different optomechanical couplings g_1. The other parameter values are the same as in Fig. 2.

IV. RESULTS AND DISCUSSIONS

We first numerically evaluate the phase quadratures of the output field, $\text{Re}(\chi)$ and $\text{Im}(\chi)$, through the corresponding output field ${}^{+}a_1$ in the optical trimer system. Figure 4 shows the absorption $\text{Re}(\chi)$ and the dispersion $\text{Im}(\chi)$ of the probe field as a function of the normalized detuning δ/ω_m with different γ_2's. Here we fix the parameter $J_2 = 0.0948\gamma_1$ and change the values of the gain γ_2 from the stable to the unstable regime. In this case the stable-unstable critical point is $\gamma_2 = 0.1\gamma_1$. The other parameter values are the same as in Fig. 2. When the gain γ_2 is small and the system is stable, i.e., $\gamma_2 < 0.1\gamma_1$ in Figs. 4(a)–4(c), the structure of the absorption shape is symmetric and the dispersion shape is antisymmetric

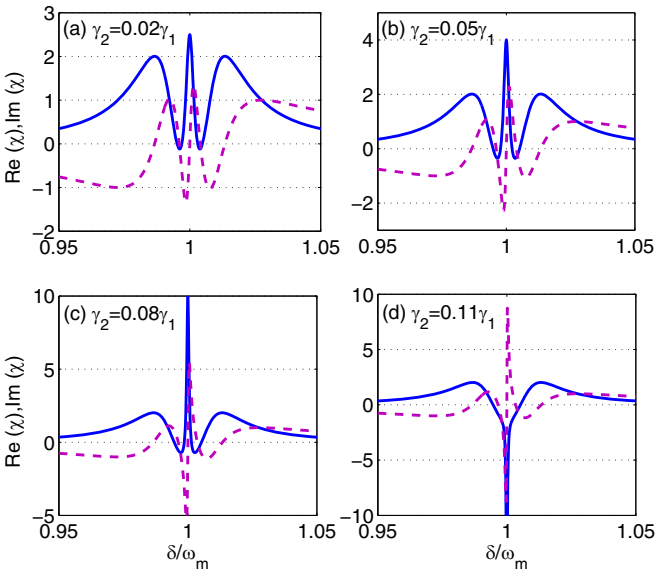

FIG. 4. The real part (blue line) and the imaginary part (purple dashed line) of the output probe field as a function of the probe detuning δ/ω_m with different γ_2's in the optical trimer system. $g_1 = 0$, $J_2 = 0.0948\gamma_1$, and the other parameter values are the same as in Fig. 2.

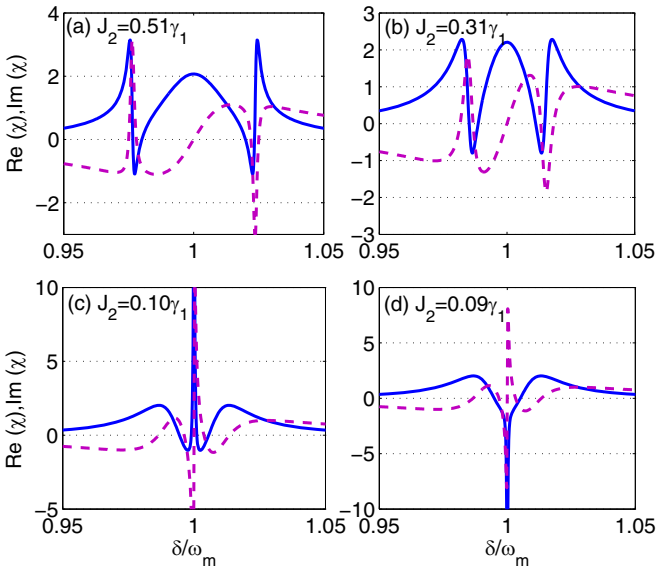

FIG. 5. The real part (blue line) and imaginary part (purple dashed line) of the output probe field as a function of the probe detuning δ/ω_m with different tunneling strengths J_2 in the optical trimer system. $g_1 = 0$, $\gamma_2 = 0.1\gamma_1$, and the other parameter values are the same as in Fig. 2.

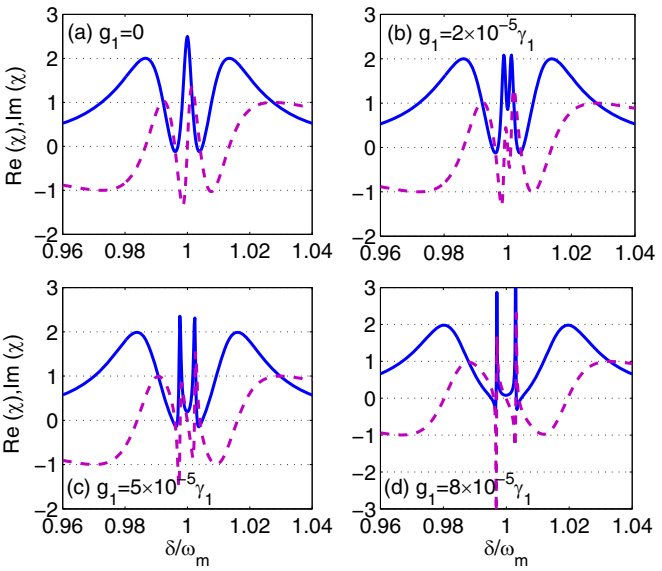

FIG. 6. The real part (blue line) and imaginary part (purple dashed line) of the output probe field as a function of the probe detuning δ/ω_m with different optomechanical coupling strengths when a mechanical oscillator is coupled to the passive cavity. $J_2 = 0.0948\gamma_1$, $\gamma_2 = 0.02\gamma_1$, and the other parameter values are the same as in Fig. 2.

near $\delta \simeq \omega_m$. Further, it is found from Figs. 4(a)–4(c) that there always exist two dips in absorption which appear on both sides of $\delta = \omega_m$. The width of each transparency window increases slightly and the distance between the transparency windows decreases slightly with increasing gain γ_2. Thus, in the stable regime of the trimer system, the transparency state is robust against the gain of the active cavity, which results from the destructive interferences among different excitation paths via the coupling between the no-loss-gain cavity and the adjacent cavities. In addition, the couplings between the cavity modes lead to three peaks of absorption, which appear respectively at $\delta = \omega_m$ and on the two sides of $\delta = \omega_m$. In the stable regime near the stable-unstable critical value, i.e., $\gamma_2 = 0.08\gamma_1$, the absorption rate of the trimer system at $\delta = \omega_m$ increases quickly with increasing gain γ_2 so that a strong resonance absorption induced by the active cavity can be attained. However, when the gain γ_2 becomes a litter larger, the trimer system will become unstable. It is found from Fig. 4(d) that in the unstable regime near the stable-unstable critical point, i.e., $\gamma_2 = 0.11\gamma_1$, the absorption profile at $\delta = \omega_m$ reverses from the peak to the dip. In particular, the dip becomes negative so that the weak probe field is amplified significantly [80,81]. Therefore, the optical properties of the system can be used for evaluating the change of an optical trimer system from the stable to the unstable regime.

We also discuss in detail the absorption and the dispersion of the probe field versus the normalized detuning δ/ω_m with different tunneling strengths J_2, as shown in Fig. 5. We fix the gain $\gamma_2 = 0.1\gamma_1$ and change the values of parameter J_2 from the stable to the unstable regime gradually. In Figs. 5(a)–5(c), it is shown that when the system is stable, i.e, $J_2 \gtrsim 0.10\gamma_1$, the distance between the left and right transparency windows increases significantly with increasing tunneling strength J_2. Thus, a large tunneling strength J_2 helps one observe the transparent behavior of the trimer system. Similarly, in the stable regime, when the tunneling strength J_2 approaches the critical value, i.e., $J_2 = 0.1\gamma_1$, a very large absorption rate of the probe field is attained at $\delta = \omega_m$. When the tunneling strength J_2 becomes a litter smaller and approaches the stable-unstable critical point in the unstable regime, i.e., $J_2 = 0.09\gamma_1$, the absorption shape at $\delta = \omega_m$ also reverses.

The optical properties of the trimer system can be changed significantly by coupling a mechanical oscillator to the passive cavity of the system, where the optomechanical interaction between the mechanical oscillator and the cavity mode leads to one additional interference channel. Correspondingly, the phenomenon of optomechanically induced transparency (OMIT) can be generated. In Fig. 6, we plot the absorption $\mathrm{Re}(\chi)$ and the dispersion $\mathrm{Im}(\chi)$ of the probe field as a function of the normalized detuning δ/ω_m in the four-mode optomechanical system. Here the parameters $\gamma_2 = 0.02\gamma_1$ and $J_2 = 0.0948\gamma_1$ in the coupled optomechanical system satisfy the stable condition, which can be seen from Fig. 3. Comparing with the optical trimer system, it is found that in the presence of the optomechanical coupling, i.e., $g_1 = 5 \times 10^{-5}\gamma_1$, a familiar transparency window induced by the optomechanical interaction occurs at $\delta = \omega_m$. The OMIT behavior in the optomechanical system results from the destructive interference between the probe field and the anti-Stokes field induced by the radiation pressure and can be understood by the optomechanical coupling between the passive cavity and the mechanical oscillator. According to Fig. 1(b), photons with frequency ω_p can be generated through four paths in the coupled optomechanical system. Specifically, when the driving field is a "red" detuning, i.e, $\Delta_1 = \omega_m$, one transition path is from the state $|n_1, n_0, n_2, n_m\rangle$ to the state $|n_1 + 1, n_0, n_2, n_m - 1\rangle$ in the passive cavity. Due to

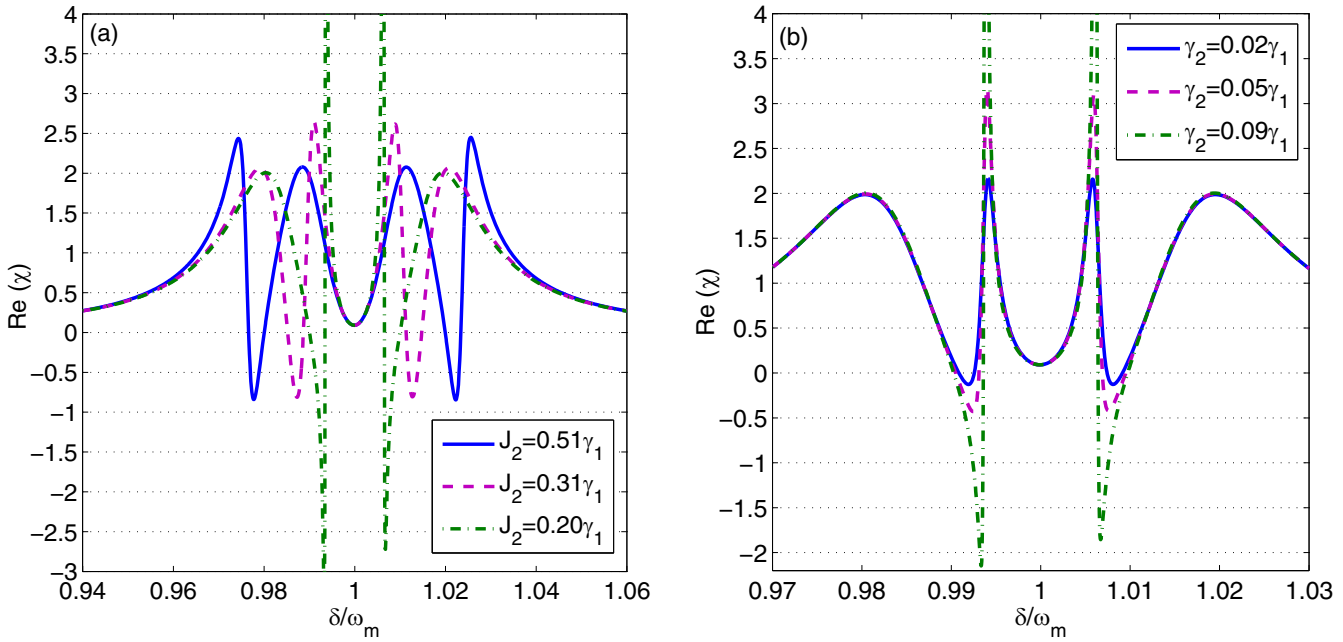

FIG. 7. The real part of the output probe field as a function of the probe detuning δ/ω_m with different J_2's and γ_2's when the mechanical oscillator is included. (a) $g_1 = 7.4 \times 10^{-5}\gamma_1$ and $\gamma_2 = 0.1\gamma_1$; (b) $g_1 = 7.4 \times 10^{-5}r_1$ and $J_2 = 0.195\gamma_1$; the other parameter values are the same as in Fig. 2.

the coupling between the passive cavity and the no-loss-gain cavity, the excited photon tunnels into the no-loss-gain cavity through the tunneling effect between them and then tunnels back to the passive cavity. Further, due to the decay of the passive cavity, the state $|n_1+1, n_0, n_2, n_m-1\rangle$ decays to the state $|n_1, n_0, n_2, n_m-1\rangle$ and emits a photon with frequency ω_p. The other path is from the state $|n_1, n_0, n_2, n_m\rangle$ to $|n_1+1, n_0, n_2, n_m-1\rangle$. Then the excited photon tunnels into the no-loss-gain cavity and the gain cavity and then tunnels back in turn to the passive cavity, which is realized by the couplings between the no-loss-gain cavity and the adjacent cavities. Finally the photon with frequency ω_p can be generated by the decay of the state $|n_1+1, n_0, n_2, n_m-1\rangle$ in the passive cavity. The third path is from the state $|n_1, n_0, n_2, n_m\rangle$ to $|n_1+1, n_0, n_2, n_m-1\rangle$ and then to the state $|n_1, n_0, n_2, n_m-1\rangle$ directly without tunneling into the no-loss-gain cavity and the gain cavity. Along with dissipation, the system emits a photon with frequency ω_p. The paths above and the probe field itself lead to a destructive interference and make the cavity transparent to the probe field.

In addition, it is noted from Fig. 6(d) that when the optomechanical coupling strength g_1 is large enough, i.e., $g_1 = 8 \times 10^{-5}\gamma_1$, the two additional peaks of absorption on the vicinity of the middle transparency window are enhanced significantly, which results from the optomechanical coupling between the mechanical oscillator and the optical trimer system. Furthermore, the distance between the two absorption windows widens with increasing coupling strength g_1. In particular, it is seen from Fig. 6 that, in the presence of the mechanical oscillator, the positions of outside round peaks of absorption depend on the coupling strength such that the distance between them increases with g_1. Consequently, the resonance absorptions can be controlled by the interaction between the mechanical oscillator and the optical trimer system.

We can investigate the influence of the gain γ_2 and the tunneling strength J_2 on the peaks of absorption of the probe field in the presence of optomechanical coupling, i.e., $g_1 = 7.4 \times 10^{-5}\gamma_1$. As shown in Fig. 7, we depicted the absorption of the probe field as a function of the normalized detuning δ/ω_m with different J_2's and γ_2's. It is found that, in the presence of the mechanical oscillator, the transparency window induced by the optomechanical coupling always appears at $\delta = \omega_m$. Also the coupling strength J_2 and the gain γ_2 do not influence the depth of the dip in absorption. However, when the coupling strength J_2 is very small and approaches the stable-unstable border, i.e., $J_2 = 0.20\gamma_1$, the positive peaks of absorption near $\delta = \omega_m$ induced by the optomechanical coupling change significantly so that the strong resonance absorption due to optomechanical coupling can be attained. Moreover, the depths of the dips in absorption near $\delta = \omega_m$ also change significantly and thus the amplification of the weak probe field is enhanced. It is shown in Fig. 7(b) that the peaks of absorption induced by the optomechanical coupling rise but the outside round peaks of absorption do not change with increasing gain γ_2. Similarly, the dips in absorption near $\delta = \omega_m$ become deeper with increasing gain γ_2 so that the amplification of the optomechanical system can be easily demonstrated. These results indicate that the optical properties of the optical trimer system can be maneuvered by coupling a mechanical oscillator to the trimer system. Apart from the tunneling strength J_2 and the gain ratio γ_2, we also investigate the effect of the driving strength Ω_d on the absorption shape of the four-mode optomechanical system. In Fig. 8, we plot the absorption $\mathrm{Re}(\chi)$ of the probe field as a function of the normalized detuning δ/ω_m with different driving strengths Ω_d. It is clearly shown that the induced transparency at $\delta = \omega_m$ appears and the separation of the split peaks increases gradually with increasing driving strength Ω_d. This is because

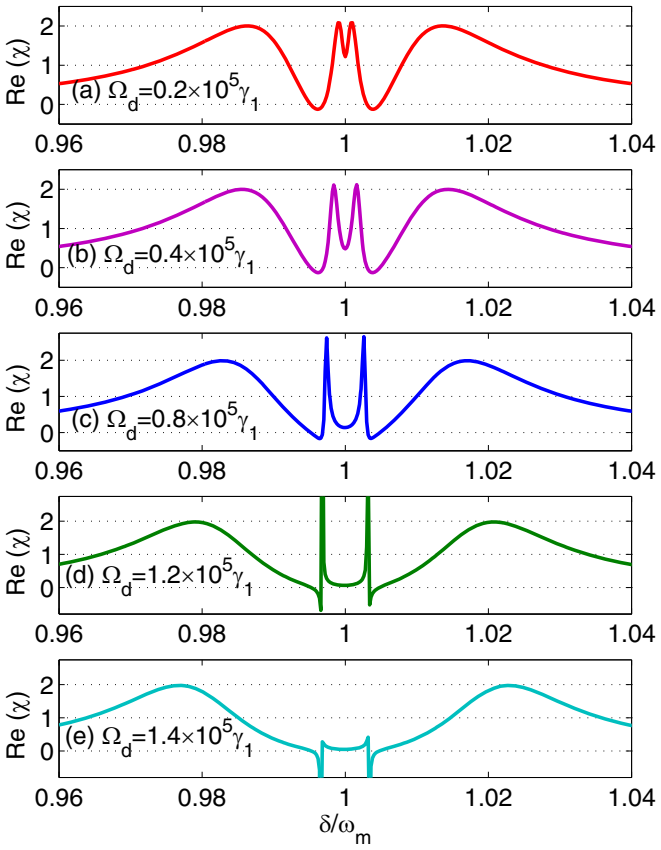

FIG. 8. The real part of the output probe field as a function of the probe detuning δ/ω_m with different driving strength Ω_d. $g_1 = 7.4 \times 10^{-5}\gamma_1$, $J_2 = 0.0948\gamma_1$, $\gamma_2 = 0.02\gamma_1$ and the other parameter values are the same as in Fig. 2.

when the driving strength of the system is increased, the effective optomechanical coupling between the mechanical oscillator and the passive cavity can be enhanced significantly, which is related to the increase of the steady-state photon number. Therefore, the OMIT behavior at $\delta = \omega_m$ can be conveniently modified by adjusting the driving strength, which is easily controlled by the laser power [82]. Due to the stability condition, there exists a critical value for the driving strength of the system. Further, we find from Fig. 8 that when Ω_d approaches the critical value, i.e., $\Omega_d \simeq 1.2 \times 10^5\gamma_1$, in Fig. 8(d), the peaks of absorption induced by the optomechanical coupling rise quickly and the dips of absorption near $\delta = \omega_m$ deepen quickly, which leads to a significant amplification of the optomechanical system. In contrast, the height of the outside round peaks of absorption induced by the coupling between the optical cavities remains unchanged but the separation increases with increasing driving strength. It is found from Fig. 8(e) that in the unstable regime near the stable-unstable critical point, i.e., $\Omega_d \simeq 1.4 \times 10^5\gamma_1$, the values of the peaks of absorption on the two sides of $\delta = \omega_m$ decrease significantly.

In order to display clearly the dependence of the peak separation and the dips of absorption on the control parameters of the system, in Fig. 9 we show the separation D_{12}/ω_m (D_{34}/ω_m) between the outside round peaks of absorption (the middle peaks of absorption) and the depths of absorption dips $\mathrm{Re}(\chi)_{\mathrm{min}}^{L,R}$ near $\delta = \omega_m$ as a function of the driving strength Ω_d, where $D_{12} = \delta_1 - \delta_2$ and δ_2 (δ_1) is the detuning corresponding to the left (right) round absorption peak in Fig. 8, and $D_{34} = \delta_3 - \delta_4$ with δ_4 and δ_3 being the detunings corresponding to the middle absorption peaks in Fig. 8. The detuning $\delta_{1,2,3,4}$ can be evaluated by $d\,\mathrm{Re}(\chi)/d\delta|_{\delta=\delta_{1,2,3,4}} = 0$. It is clearly seen from Fig. 9(a) that D_{12} and D_{34} increase nonlinearly with increasing driving strength. The maxima of D_{12} and D_{34} corresponding to the critical driving strength are $0.0435\omega_m$ and $0.0065\omega_m$ with the selected parameters, respectively. Further, we can see clearly from Fig. 9(b) that with an increase of the driving strength, the depths of the absorption dips near $\delta = \omega_m$ decrease slowly at first, and then decline rapidly from $\mathrm{Re}(\chi)_{\mathrm{min}} \simeq -0.5$ to $\mathrm{Re}(\chi)_{\mathrm{min}} \simeq -5$ in the region next to the stable-unstable critical value. These characteristics of the system mean that the dips of absorption

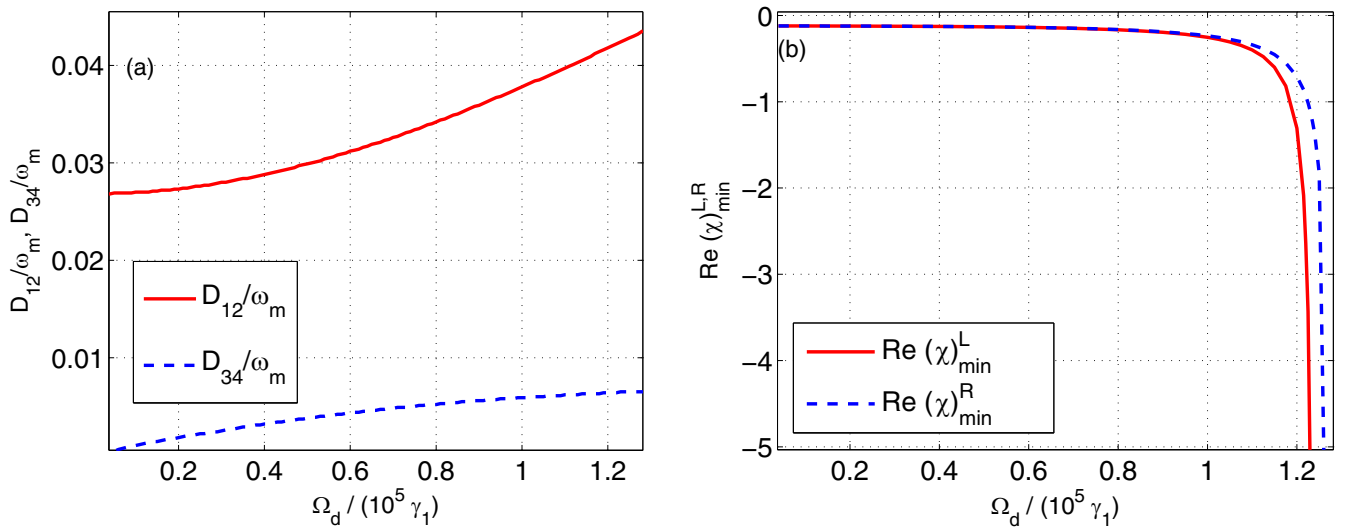

FIG. 9. The separations D_{12}/ω_m and D_{34}/ω_m between the peaks of absorption (a) and the depths of absorption dips $\mathrm{Re}(\chi)_{\mathrm{min}}^{L,R}$ on the left or the right side $\delta = \omega_m$ (b) are plotted as a function of the driving strength Ω_d. Other parameter values are the same as in Fig. 8.

induced by the coupling between the optical cavities can be changed significantly by the driving strength of the system, which determines the effective coupling between the mechanical oscillator and the optical cavity.

V. CONCLUSIONS

In conclusion, we propose a hybrid four-mode coupled optomechanical system consisting of an array of three single-mode cavities and a mechanical oscillator to investigate the change of the optical properties of the optical trimer system brought about by the mechanical oscillator. We first analyze the stable and the unstable regimes of the system in the presence and absence of the optomechanical coupling by numerically calculating the Lyapunov exponents of the system. It is found that the stable regime of the coupled optomechanical system appears when the gain-to-loss ratio is small. Then, we investigate the optical response of the trimer system by changing the gain of the active cavity and the tunneling strengths between the adjacent cavities. It is clearly seen that due to destructive interferences among the excitation paths of three single-mode cavities, there exist three absorption peaks and two dips in absorption. Especially, the trimer system has a strong resonance absorption in the stable regime near the stable-unstable critical value and then amplifies quickly in the unstable regime. Further, we investigate the optical properties of a four-mode optomechanical system by disposing a mechanical oscillator to couple the passive cavity. Comparing it with the optical trimer system, we find that the anti-Stokes field caused by the optomechanical coupling induces an additional optomechanical transparent behavior at $\delta = \omega_m$ as well as the corresponding resonance peaks of absorption beside $\delta = \omega_m$, which depend on the optomechanical coupling, the tunneling strengths between the optical cavities, and the gain of the active cavity. In contrast, the transparent behavior at $\delta = \omega_m$ does not change with different gain ratios γ_2 and tunneling strengths J_2. We also discuss in detail the effect of the driving strength Ω_d on the absorption shape of the four-mode optomechanical system. It is shown that the distance between the split peaks goes up with increasing driving strength Ω_d. When Ω_d approaches the stable-unstable critical value, the depths of absorbtion dips near $\delta = \omega_m$ decline rapidly. These results present interesting optical-response properties of an optical trimer system induced by the coupling to a mechanical oscillator, which provide a potential application in effectively manipulating the propagation of light with more handles.

ACKNOWLEDGMENTS

W.J.N. is supported by the National Natural Science Foundation of China (NSFC) under Grant No. 11565014 and the Natural Science Foundation of Jiangxi Province under Grant No. 20171BAB201015. A.X.C. is supported by the NSFC under Grant No. 11365009. Y.H.L. is supported by the NSFC under Grants No. 11375093 and No. 11775035.

[1] M. Aspelmeyer, T. J. Kippenberg, and F. Marquardt, Rev. Mod. Phys. **86**, 1391 (2014).
[2] M. Aspelmeyer, P. Meystre, and K. Schwab, Phys. Today **65**, 29 (2012).
[3] F. Marquardt and S. M. Girvin, Physics **2**, 40 (2009).
[4] Q. Zheng, J. Xu, Y. Yao, and Y. Li, Phys. Rev. A **94**, 052314 (2016).
[5] X. Li, W. Nie, A. Chen, and Y. Lan, Phys. Rev. A **96**, 063819 (2017).
[6] D. Vitali, S. Gigan, A. Ferreira, H. R. Böhm, P. Tombesi, A. Guerreiro, V. Vedral, A. Zeilinger, and M. Aspelmeyer, Phys. Rev. Lett. **98**, 030405 (2007).
[7] X. Yang, Y. Ling, X. Shao, and M. Xiao, Phys. Rev. A **95**, 052303 (2017).
[8] J. D. Teufel, T. Donner, D. Li, J. W. Harlow, M. S. Allman, K. Cicak, A. J. Sirois, J. D. Whittaker, K. W. Lehnert, and R. W. Simmonds, Nature (London) **475**, 359 (2011).
[9] J. Chan, T. P. M. Alegre, A. H. Safavi-Naeini, J. T. Hill, A. Krause, S. Gröblacher, A. Markus, and O. Painter, Nature (London) **478**, 89 (2011).
[10] M. Bhattacharya and P. Meystre, Phys. Rev. Lett. **99**, 073601 (2007).
[11] W. Nie, A. Chen, and Y. Lan, Opt. Express **23**, 30970 (2015).
[12] X. Chen, Y. C. Liu, P. Peng, Y. Zhi, and Y. F. Xiao, Phys. Rev. A **92**, 033841 (2015).
[13] M. Ludwig, A. H. Safavi-Naeini, O. Painter, and F. Marquardt, Phys. Rev. Lett. **109**, 063601 (2012).
[14] K. Stannigel, P. Komar, S. J. M. Habraken, S. D. Bennett, M. D. Lukin, P. Zoller, and P. Rabl, Phys. Rev. Lett. **109**, 013603 (2012).
[15] P. Komar, S. D. Bennett, K. Stannigel, S. J. M. Habraken, P. Rabl, P. Zoller, and M. D. Lukin, Phys. Rev. A **87**, 013839 (2013).
[16] X. Y. Lü, W. M. Zhang, S. Ashhab, Y. Wu, and F. Nori, Sci. Rep. **3**, 2943 (2013).
[17] K. Børkje, A. Nunnenkamp, J. D. Teufel, and S. M. Girvin, Phys. Rev. Lett. **111**, 053603 (2013).
[18] M. A. Lemonde, N. Didier, and A. A. Clerk, Phys. Rev. Lett. **111**, 053602 (2013).
[19] H. Suzuki, E. Brown, and R. Sterling, Phys. Rev. A **92**, 033823 (2015).
[20] I. M. Mirza and S. J. van Enk, Phys. Rev. A **90**, 043831 (2014).
[21] I. M. Mirza, J. Opt. Soc. Am. B **32**, 1604 (2015).
[22] S. Weis, R. Rivière, S. Deléglise, E. Gavartin, O. Arcizet, A. Schliesser, and T. J. Kippenberg, Science **330**, 1520 (2010).
[23] G. S. Agarwal and S. Huang, Phys. Rev. A **81**, 041803 (2010).
[24] A. H. Safavi-Naeini, T. P. Mayer Alegre, J. Chan, M. Eichenfield, M. Winger, Q. Lin, J. T. Hill, D. E. Chang, and O. Painter, Nature (London) **472**, 69 (2011).
[25] M. Karuza, C. Biancofiore, M. Bawaj, C. Molinelli, M. Galassi, R. Natali, P. Tombesi, G. Di Giuseppe, and D. Vitali, Phys. Rev. A **88**, 013804 (2013).
[26] H. Xiong, L. G. Si, A. S. Zheng, X. Yang, and Y. Wu, Phys. Rev. A **86**, 013815 (2012).

[27] P. C. Ma, J. Q. Zhang, Y. Xiao, M. Feng, and Z. M. Zhang, Phys. Rev. A **90**, 043825 (2014).
[28] K. Qu and G. S. Agarwal, Phys. Rev. A **87**, 031802 (2013).
[29] B. P. Hou, L. F. Wei, and S. J. Wang, Phys. Rev. A **92**, 033829 (2015).
[30] X. Y. Zhang, Y. Q. Guo, P. Pei, and X. X. Yi, Phys. Rev. A **95**, 063825 (2017).
[31] S. E. Harris, J. E. Field, and A. Imamoğlu, Phys. Rev. Lett. **64**, 1107 (1990).
[32] S. E. Harris, Phys. Today **50**(7), 36 (1997).
[33] C. Jiang, H. Liu, Y. Cui, X. Li, G. Chen, and B. Chen, Opt. Express **21**, 12165 (2013).
[34] A. Lezama, S. Barreiro, and A. M. Akulshin, Phys. Rev. A **59**, 4732 (1999).
[35] A. Lipsich, S. Barreiro, A. M. Akulshin, and A. Lezama, Phys. Rev. A **61**, 053803 (2000).
[36] A. V. Taichenachev, A. M. Tumaikin, and V. I. Yudin, Phys. Rev. A **61**, 011802 (1999).
[37] F. Hocke, X. Zhou, A. Schliesser, T. J. Kippenberg, H. Huebl, and R. Gross, New J. Phys. **14**, 123037 (2012).
[38] X. Zhang, N. Xu, K. Qu, Z. Tian, R. Singh, J. Han, G. S. Agarwal, and W. Zhang, Sci. Rep. **5**, 10737 (2015).
[39] K. A. Yasir and W. M. Liu, Sci. Rep. **6**, 22651 (2016).
[40] D. E. Chang, A. H. Safavi-Naeini, M. Hafezi, and O. Painter, New J. Phys. **13**, 023003 (2011).
[41] V. Fiore, Y. Yang, M. C. Kuzyk, R. Barbour, L. Tian, and H. Wang, Phys. Rev. Lett. **107**, 133601 (2011).
[42] B. Chen, C. Jiang, and K. D. Zhu, Phys. Rev. A **83**, 055803 (2011).
[43] M. J. Akram, M. M. Khan, and F. Saif, Phys. Rev. A **92**, 023846 (2015).
[44] V. Fiore, C. Dong, M. C. Kuzyk, and H. Wang, Phys. Rev. A **87**, 023812 (2013).
[45] J. Q. Zhang, Y. Li, M. Feng, and Y. Xu, Phys. Rev. A **86**, 053806 (2012).
[46] G. S. Agarwal and S. Huang, Phys. Rev. A **85**, 021801 (2012).
[47] Y. Liu, M. Davanco, V. Aksyuk, and K. Srinivasan, Phys. Rev. Lett. **110**, 223603 (2013).
[48] Q. Wang, Y. H. Zhao, Z. He, and C. M. Yao, Int. J. Theor. Phys. **55**, 1324 (2016).
[49] A. Kronwald and F. Marquardt, Phys. Rev. Lett. **111**, 133601 (2013).
[50] T. Ramos, V. Sudhir, K. Stannigel, P. Zoller, and T. J. Kippenberg, Phys. Rev. Lett. **110**, 193602 (2013).
[51] J. M. Pirkkalainen, S. U. Cho, F. Massel, J. Tuorila, T. T. Heikkilä, P. J. Hakonen, and M. A. Sillanpää, Nat. Commun. **6**, 6981 (2015).
[52] I. M. Mirza, Opt. Lett. **41**, 2422 (2016).
[53] L. Li, W. Nie, and A. Chen, Sci. Rep. **6**, 35090 (2016).
[54] W. Nie, A. Chen, and Y. Lan, Phys. Rev. A **93**, 023841 (2016).
[55] W. Nie, A. Chen, and Y. Lan, Opt. Express **25**, 32931 (2017).
[56] C. Jiang, L. N. Song, and Y. Li, Phys. Rev. A **97**, 053812 (2018).
[57] X. Z. Zhang, L. Tian, and Y. Li, Phys. Rev. A **97**, 043818 (2018).
[58] X. W. Xu, Y. J. Li, and Y. X. Liu, Phys. Rev. A **87**, 025803 (2013).
[59] Y. X. Liu, X. W. Xu, A. Miranowicz, and F. Nori, Phys. Rev. A **89**, 043818 (2014).
[60] C. G. Alzar, M. Martinez, and P. Nussenzveig, Am. J. Phys. **70**, 37 (2002).
[61] C. Dong, V. Fiore, M. C. Kuzyk, and H. Wang, Phys. Rev. A **87**, 055802 (2013).
[62] K. Totsuka, N. Kobayashi, and M. Tomita, Phys. Rev. Lett. **98**, 213904 (2007).
[63] L. F. Xue, Z. R. Gong, H. B. Zhu, and Z. H. Wang, Opt. Express **25**, 17249 (2017).
[64] A. Sohail, Y. Zhang, J. Zhang, and C. S. Yu, Sci. Rep. **6**, 28830 (2016).
[65] F. C. Lei, M. Gao, C. Du, Q. L. Jing, and G. L. Long, Opt. Express **23**, 11508 (2015).
[66] C. Bai, B. P. Hou, D. G. Lai, and D. Wu, Phys. Rev. A **93**, 043804 (2016).
[67] M. A. Lemonde, N. Didier, and A. A. Clerk, Nat. Commun. **7**, 11338 (2016).
[68] Z. Liu, Y. C. Lai, and M. A. Matias, Phys. Rev. E **67**, 045203 (2003).
[69] L. Lü, C. Li, S. Liu, Z. Wang, J. Tian, and J. Gu, Nonlinear Dyn. **81**, 801 (2015).
[70] L. Lü, M. Yu, L. L. Wei, M. Zhang, and Y. S. Li, Chin. Phys. B **21**, 100507 (2012).
[71] W. Li, C. Li, and H. Song, Phys. Lett. A **380**, 672 (2016).
[72] M. Eichenfield, J. Chan, R. M. Camacho, K. J. Vahala, and O. Painter, Nature (London) **462**, 78 (2009).
[73] B. Peng, Ş. K. Özdemir, F. Lei, F. Monifi, M. Gianfreda, G. L. Long, S. Fan, F. Nori, C. M. Bender, and L. Yang, Nat. Phys. **10**, 394 (2014).
[74] W. Li, Y. Jiang, C. Li, and H. Song, Sci. Rep. **6**, 31095 (2016).
[75] M. Eichenfield, R. Camacho, J. Chan, K. J. Vahala, and O. Painter, Nature (London) **459**, 550 (2009).
[76] X. Y. Lü, H. Jing, J. Y. Ma, and Y. Wu, Phys. Rev. Lett. **114**, 253601 (2015).
[77] L. Chang, X. Jiang, S. Hua, C. Yang, J. Wen, L. Jiang, G. Li, G. Wang, and M. Xiao, Nat. Photon. **8**, 524 (2014).
[78] H. Wang, H. C. Sun, J. Zhang, and Y. X. Liu, Sci. China Phys. Mech. Astron. **55**, 2264 (2012).
[79] W. Li, C. Li, and H. Song, Phys. Rev. A **95**, 023827 (2017).
[80] F. Massel, T. T. Heikkilä, J. M. Pirkkalainen, S. U. Cho, H. Saloniemi, P. J. Hakonen, and M. A. Sillanpää, Nature (London) **480**, 351 (2011).
[81] W. Z. Jia, L. F. Wei, Y. Li, and Y. X. Liu, Phys. Rev. A **91**, 043843 (2015).
[82] H. Xiong and Y. Wu, Appl. Phys. Rev. **5**, 031305 (2018).